

Hysteresis and intermittency in a nano-bridge based suspended DC-SQUID

Eran Segev, Oren Suchoi, Oleg Shtempluck, Fei Xue,* and Eyal Buks
Department of electrical engineering, Technion, Haifa 32000, Israel

(Dated: November 8, 2018)

We study voltage response of nano-bridge based DC-SQUID fabricated on a Si_3N_4 membrane. Such a configuration may help in reducing $1/f$ noise, which originates from substrate fluctuating defects. We find that the poor thermal coupling between the DC-SQUID and the substrate leads to strong hysteretic response of the SQUID, even though it is biased by an alternating current. In addition, when the DC-SQUID is biased near a threshold of spontaneous oscillations, the measured voltage has an intermittent pattern, which depends on the applied magnetic flux through the SQUID.

PACS numbers:

Superconducting quantum interference devices (SQUIDs) are key components in many applications [1]. One of the major research goals with SQUIDs nowadays is to reduce noises in the Josephson junctions (JJs) composing the SQUIDs. This issue was extensively studied in the past decades, where it was shown that one of the main sources of noise is the coupling of the JJs to the substrate, which induces $1/f$ noises [2]. Several studies have tried to solve this problem by suspending the JJs and thus decouple them from the substrate. So far these studies have only shown moderate success [3–5]. Another emerging technology, which attracts an increasing interest, is SQUIDs based on nano-bridge weak-links. Such SQUIDs can be made extremely small and have the potential to outperform conventional SQUIDs in terms of noise properties [6, 7].

Our original research goal was to study noise properties of a nano-bridge based DC-SQUIDs suspended on a Silicon Nitride (Si_3N_4) membrane. However, we discovered that non-equilibrium thermal processes, which emerge due to the poor coupling of the JJs to the substrate, play a dominant role in SQUIDs dynamics. When the SQUID is excited by alternating current strong hysteretic response of the DC-SQUID is observed, even though such excitation should, in principle, eliminate hysteretic behavior. In addition, when the SQUID is biased near a threshold of spontaneous oscillations, the measured voltage shows an intermittent pattern, which depends on the magnetic flux through the SQUID. To account for these results we extend the theoretical model in Ref. [8] to include low frequency variations in the SQUID temperature. Numerical simulations show qualitative agreement with the experimental data.

A simplified circuit layout of a typical device is illustrated in Fig. 1(b). We build our devices on a high resistivity Silicon wafer, covered by a 100 nm-thick layer of Si_3N_4 . A small section of the wafer is etched from the back to produce a suspended Si_3N_4 membrane, having size of $100 \mu\text{m}^2$. The DC-SQUID is made of Niobium, having layer thickness of 80 nm and lateral dimensions of

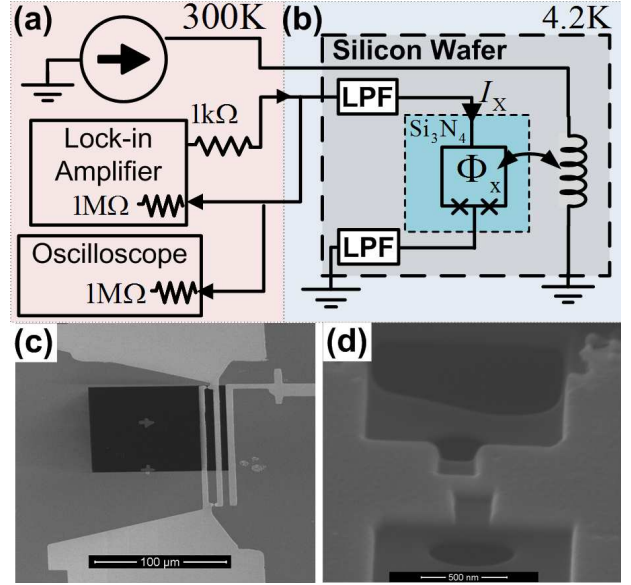


FIG. 1: (Color online) (a) Measurement setup. (b) A simplified circuit layout for a DC-SQUID. (c) Electron micrograph of a DC-SQUID partially fabricated on top a Si_3N_4 membrane. (d) Electron micrograph image of a nano-bridge.

$110 \times 7 \mu\text{m}^2$. The self-inductance of the SQUID is calculated using FastHenry program [9] to be $L = 100\text{pH}$. The DC-SQUID is composed of two nano-bridge JJs (NBJJs), one NBJJ in each of its two arms. The dimensions of the bridges are $100 \times 115 \text{nm}^2$, and their combined critical current is 1.2 mA. Most of the SQUID structure, including one of the NBJJs is fabricated on the Si_3N_4 membrane, as shown by the electron micrographs in subfigures 1(c) and 1(d). An on-chip stripline passes nearby the DC-SQUID, and is used to generate magnetic flux in the DC-SQUID loop. A DC bias line, which includes on-chip low-pass filters (LPFs), is connected to the DC-SQUID and is used for voltage measurements of the SQUID. Note that the DC-SQUID is embedded in a superconducting stripline resonator (not illustrated in Fig. 1(b)), but the resonator was not used in the experiments, and thus had a negligible influence on the experiments presented in this

*Current affiliation: Department of Physics, University of Basel.

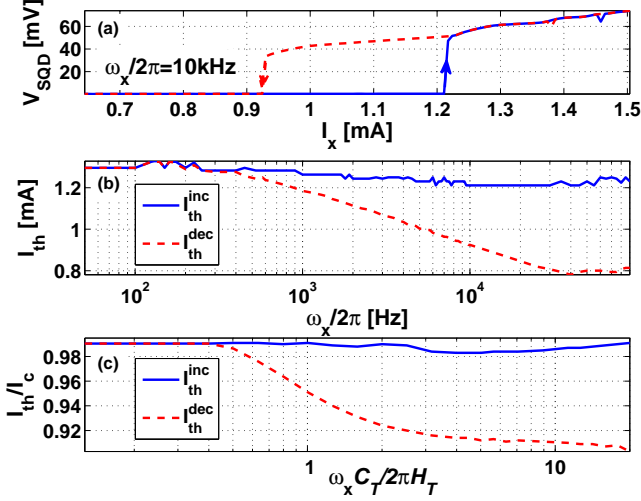


FIG. 2: Hysteretic current-voltage measurements. Panel (a) shows DC-SQUID voltage traces measured for increasing and decreasing current excitation sweeps. Panels (b) and (c) show measurement and simulation results, respectively, of increasing and decreasing threshold currents as a function of the excitation frequency.

paper. Further design considerations and fabrication details can be found elsewhere [10, 11].

Our experiments are carried out using the setup depicted in Fig. 1(a). We use a lock-in amplifier, which applies alternating current through the SQUID. The excitation frequencies can be up to 100 kHz. We measure the voltage across the DC-SQUID using the lock-in amplifier and record its time domain dynamics using an oscilloscope. In experiments showing intermittency we also apply DC magnetic flux through the SQUID. All measurements are carried out while the device is fully immersed in liquid Helium.

Figure 2(a) shows an example of the DC-SQUID hysteretic response to an excitation current having alternating frequency of $\omega_x/2\pi = 10$ kHz. This measurement shows the measured voltage across the SQUID when the current amplitude is swept up and then down. Each recorded point is averaged over 100 ms, thus including 1000 excitation cycles. Such alternating excitation should, in principle, eliminate hysteresis in the response of the DC-SQUID, provided that all characteristic time scales of the device are much shorter than the excitation period. Note that, the thermal relaxation rate of a local hot-spot, created in a nano-bridge having good thermal coupling to the substrate, is typically on the order of gigahertz [12]. In contrary to our expectation, the measurement of hysteretic current-voltage characteristic behavior under alternating current excitation indicates that, there is a much longer characteristic thermal time-scale, on the order of millisecond, which affects the DC-SQUID dynamics. Such a long time-scale may exist in our device because the Si_3N_4 membrane, to which

the SQUID is coupled, has relatively large heat capacity, and also because of the poor coupling between this membrane and its surrounding, which results in a relatively long thermal relaxation time.

Figure 2(b) summarizes several measurements like the one shown in Fig. 2(a). It plots the increasing and decreasing threshold currents (i.e. the values of applied currents corresponding to voltage jumps in the increasing and decreasing current sweeps respectively) as a function of the lock-in amplifier carrier frequency. These threshold currents are approximately equal one another only up to frequencies of about 500 Hz. The hysteretic nature of the DC-SQUID emerges when the excitation frequency further increases. The decreasing threshold current falls to lower values while the increasing one only slightly degraded. This trend continues up to frequencies of about 40 kHz, where both threshold currents cease to depend on the excitation frequency.

In order to account for the above results, we extend the model in Ref. [8] of hysteretic, metastable DC-SQUID to include slow variations of the SQUID temperature. According to the model, the equations of motion DC-SQUID are the following two equations for the NBJJs phases γ_1 and γ_2

$$\begin{aligned} \dot{\gamma}_1 + \beta_D \dot{\gamma}_1 + (1 + \alpha_0) y(\Theta) \sin \gamma_1 \\ + \frac{1}{\beta_{L0}} (\gamma_1 - \gamma_2 + 2\pi\Phi_x/\Phi_0) = I_x/I_{c0} + g_n, \end{aligned} \quad (1)$$

$$\begin{aligned} \dot{\gamma}_2 + \beta_D \dot{\gamma}_2 + (1 - \alpha_0) y(\Theta) \sin \gamma_2 \\ - \frac{1}{\beta_{L0}} (\gamma_1 - \gamma_2 + 2\pi\Phi_x/\Phi_0) = I_x/I_{c0} + g_n, \end{aligned} \quad (2)$$

where the overdot denotes a derivative with respect to a normalized time parameter $\tau = \omega_{pl}t$, where ω_{pl} is the DC-SQUID plasma frequency. In addition, I_x is the bias current, Φ_x is the external magnetic flux, Φ_0 is flux quantum, β_D is the dimensionless damping coefficient, and E_0 is the Josephson energy. The critical current of the DC-SQUID is temperature dependant, thus we employ the notation I_{c0} for the SQUID critical current at the base temperature T_0 , defined by the coolant. The dimensionless parameters β_{L0} and α_0 characterize the DC-SQUID hysteresis and asymmetry at the base temperature T_0 , respectively. The dimensionless factor g_n is a noise term, which is neglected in our numerical calculations.

Assuming that, the temperature of the SQUID, T , has no spatial dependence. The term $y(\Theta)$ expresses the dependence of the NBJJs critical currents on the temperature. It is given by $y(\Theta) \equiv \tilde{y}(\Theta)/\tilde{y}(\Theta_0)$ [13], where $\Theta = T/T_c$, $\Theta_0 = T_0/T_c$, and T_c is the critical temperature of the DC-SQUID. The function \tilde{y} is given by $\tilde{y}(\Theta) = (1 - \Theta^2)^{3/2} (1 + \Theta^2)^{1/2}$. Using the notation $\beta_C = 2\pi C_T T_c / \Phi_0 I_{c0}$ and $\beta_H = H_T / C_T \omega_{pl}$, where C_T is thermal heat capacity and H_T is heat transfer rate, the SQUID heat balance equation reads

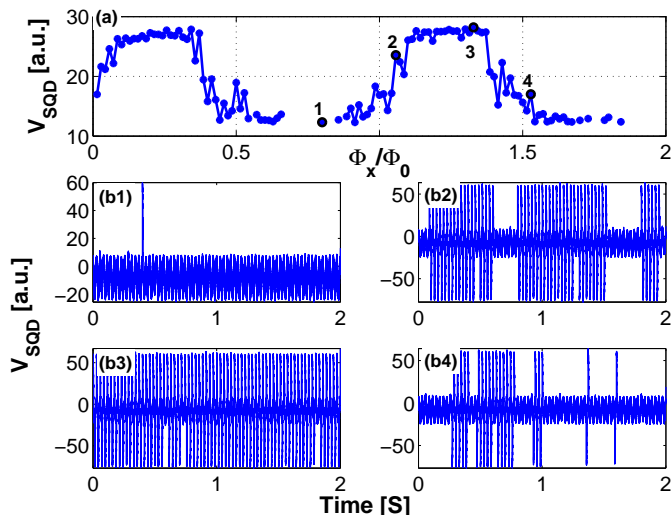


FIG. 3: Intermittent behavior. (a) Measured average squared voltage of the DC-SQUID. (b*i*) Time traces of the DC-SQUID voltage taken at the working points marked by the corresponding number *i* in panel (a).

$$\dot{\Theta} = \frac{\beta_D}{\beta_C} (\dot{\gamma}_1^2 + \dot{\gamma}_2^2) - \beta_H (\Theta - \Theta_0), \quad (3)$$

Simulation results showing the dependence of the hysteretic behavior of the DC-SQUID on the excitation frequency are shown in Fig. 2(c). This panel shows the increasing and decreasing threshold currents as a function of the excitation frequency, normalized by the thermal relaxation time. These results show qualitative agreement with the corresponding experimental results shown in Fig. 2(b).

Figure 3 shows intermittent behavior of the SQUID. In this measurement the DC-SQUID is biased near the threshold of spontaneous oscillations using alternating current having frequency of $\omega_x/2\pi = 70$ Hz. The volt-

age across the SQUID is measured as a function of time for various values of magnetic flux applied through the SQUID. Panel (a) shows the average value of the squared voltage versus the magnetic flux. Panels (b*i*) show voltage time traces measured for the corresponding marked points in panel (a). The low amplitude voltage oscillations are measured due to the existence of a parasitic serial resistance in the measurement wiring. Each time the alternating current drives the SQUID into the oscillatory zone it responds with a voltage spike measured on top of the low amplitude parasitic voltage. Spikes can be positive or negative depending on the polarity of the driving current. The measured traces show intermittent behavior, in which the spikes are generated in bunches. This behavior suggests that in this region the system becomes thermally bistable. The bistability is realized by switching between the cold locally stable state, where the DC-SQUID is in the superconducting state, and the hot locally stable state, where the SQUID becomes normal. Switching between these states is randomly triggered by external noise.

In conclusion, we have studied nano-bridge based DC-SQUIDS fabricated on a Si_3N_4 membrane. We find that the response of the DC-SQUID to a low frequency alternating excitation current is hysteretic, and that the strength of the hysteresis depends on the excitation frequency. In addition, when the SQUID is biased near a threshold of spontaneous oscillations, the measured voltage has an intermittent pattern, which depends on the applied magnetic flux through the SQUID. Such hysteretic response degrades the performance of the suspended SQUID, and questions the effectiveness of using suspension as a method for noise reduction.

E.S. is supported by the Adams Fellowship Program of the Israel Academy of Sciences and Humanities. This work is supported by the German Israel Foundation under grant 1-2038.1114.07, the Israel Science Foundation under grant 1380021, the Deborah Foundation, Russell Berrie nanotechnology institute, Israeli Ministry of Science, the European STREP QNEMS project, and MAFAT.

-
- [1] J. Clarke and A. I. Braginski, *The SQUID Handbook: Fundamentals and Technology of SQUIDS and SQUID Systems* (Wiley-VCH, 2004), 1st ed., ISBN 3527402292.
- [2] A. B. Zorin, F.-J. Ahlers, J. Niemeyer, T. Weimann, H. Wolf, V. A. Krupenin, and S. V. Lotkhov, *Phys. Rev. B* **53**, 13682 (1996).
- [3] V. A. Krupenin, D. E. Presnov, M. N. Savvateev, H. Scherer, A. B. Zorin, and J. Niemeyer, *Journal of Applied Physics* **84**, 3212 (1998).
- [4] V. A. Krupenin, D. E. Presnov, A. B. Zorin, and J. Niemeyer, *Journal of Low Temperature Physics* **118**, 287 (2000).
- [5] T. F. Li, Y. A. Pashkin, O. Astafiev, Y. Nakamura, J. S. Tsai, and H. Im, *Applied Physics Letters* **91**, 033107 (pages 3) (2007).
- [6] R. Vijay, E. M. Levenson-Falk, D. H. Slichter, and I. Siddiqi, *Applied Physics Letters* **96**, 223112 (2010).
- [7] R. Vijay, J. D. Sau, M. L. Cohen, and I. Siddiqi, *Phys. Rev. Lett.* **103**, 087003 (2009).
- [8] E. Segev, O. Suchoi, O. Shtempluck, F. Xue, and E. Buks, arXiv:1007.5225v1 (2010).
- [9] *Fast field solvers*, <http://www.fastfieldsolvers.com/>.
- [10] E. Segev, O. Suchoi, O. Shtempluck, and E. Buks, *Applied Physics Letters* **95**, 152509 (2009).
- [11] O. Suchoi, B. Abdo, E. Segev, O. Shtempluck, M. P. Blencowe, and E. Buks, *Phys. Rev. B* **81**, 174525 (2010).
- [12] M. Tarkhov, J. Claudon, J. P. Poizat, A. Korneev, A. Divochiy, O. Minaeva, V. Seleznev, N. Kaurova,

- B. Voronov, A. V. Semenov, et al., Applied Physics Letters **92**, 241112 (2008).
- [13] W. J. Skocpol, Phys. Rev. B **14**, 1045 (1976).